A novel nematode species from the Siberian permafrost shares adaptive mechanisms for cryptobiotic survival with *C. elegans* dauer larva

Anastasia Shatilovich[1#], Vamshidhar R. Gade[2,9#], Martin Pippel[3], Tarja T. Hoffmeyer[4], Alexei V. Tchesunov[5], Lewis Stevens[6], Sylke Winkler[2,7], Graham M. Hughes[8], Sofia Traikov[2], Michael Hiller[3,10], Elizaveta Rivkina[1], Philipp H. Schiffer[4*], Eugene W Myers[3], Teymuras V. Kurzchalia[2*]

1. Institute of Physicochemical and Biological Problems in Soil Science RAS, Pushchino, Russia
2. Max Planck Institute for Molecular Cell Biology and Genetics, Dresden, Germany
3. Center for Systems Biology, Dresden, Germany
4. Institute for Zoology, University of Cologne
5. Department of Invertebrate Zoology, Faculty of Biology, M.V. Lomonosov Moscow State University, Moscow, Russia
6. Tree of Life, Wellcome Sanger Institute, Cambridge, UK
7. DRESDEN concept Genome Center, Dresden, Germany
8. School of Biology and Environmental Science, University College Dublin, Belfield, Dublin, Ireland
9. Institute of Biochemistry, ETH Zürich, 8093 Zürich, Switzerland
10. LOEWE Centre for Translational Biodiversity Genomics, Senckenberg Society for Nature Research & Goethe University, Frankfurt am Main, Germany

[#] A.S and V.G contributed equally to this work

*To whom correspondence may be addressed

Email: kurzchalia@mpi-cbg.de

p.schiffer@uni-koeln.de

Abstract

Some organisms in nature have developed the ability to enter a state of suspended metabolism called cryptobiosis[1] when environmental conditions are unfavorable. This state-transition requires the execution of complex genetic and biochemical programs[1,2,3], that enables the organism to survive for prolonged periods. Recently, nematode individuals have been reanimated from Siberian permafrost after remaining in cryptobiosis. Preliminary analysis indicates that these nematodes belong to the genera *Panagrolaimus* and *Plectus*[4]. Here, we present precise radiocarbon dating indicating that the *Panagrolaimus* individuals have remained in cryptobiosis since the late Pleistocene (~46,000 years). Phylogenetic inference based on our genome assembly and a detailed morphological analysis demonstrate that they belong to an undescribed species, which we named *Panagrolaimus kolymaensis*. Comparative genome analysis revealed that the molecular toolkit for cryptobiosis in *P. kolymaensis* and in *C. elegans* is partly orthologous. We show that biochemical mechanisms employed by these two species to survive desiccation and freezing under laboratory conditions are similar. Our experimental evidence also reveals that *C. elegans* dauer larvae can remain viable for longer periods in suspended animation than previously reported. Altogether, our findings demonstrate that nematodes evolved mechanisms potentially allowing them to suspend life over geological time scales.

Introduction

Organisms from diverse taxonomic groups can survive extreme environmental conditions, such as the complete absence of water or oxygen, high temperature, freezing, or extreme salinity. The survival strategies of such organisms include a state known as suspended animation or cryptobiosis, in which they reduce metabolism to an undetectable level[6]. Spectacular examples of long-term cryptobiosis include a *Bacillus* spore that was preserved in the abdomen of bees buried in amber for 25 to 40 million years[7], and a 1000 to 1500 years-old *Lotus* seed, found in an ancient lake, that was subsequently able to germinate[8]. Metazoans such as tardigrades, rotifers and nematodes are also known for remaining in cryptobiosis for prolonged periods[9,10]. The longest records of cryptobiosis in nematodes are reported for the Antarctic species *Plectus murrayi*[11] (25.5 years in moss frozen at -20°C), and *Tylenchus polyhypnus*[12] (39 years desiccated in a herbarium specimen).

Intensive research during the last decades has demonstrated that permafrosts (perennially frozen sediments) are unique ecosystems preserving life forms at sub-zero temperatures over thousands of years[13,14,15,16]. Permafrost remains are an exceptional source for discovering a wide variety of unicellular and multicellular living organisms surviving in cryptobiosis for prolonged periods[6,17,18]. We recently reanimated soil nematodes that were preserved in Siberian permafrost for potentially thousands of years, and initial morphological observations provisionally described them as belonging to the genera *Panagrolaimus* and *Plectus.* Previous studies demonstrated several species of *Panagrolaimus* can undergo cryptobiosis in the form of anhydrobiosis (through desiccation) and cryobiosis (through freezing)[19,20,21,22,23]. In various nematodes, entry into anhydrobiosis is often accompanied by a preparatory phase of exposure to mild desiccation, known as preconditioning[21,24]. This induces a specific remodelling of the transcriptome, the proteome, and metabolic pathways that enhances survival ability[2,3,25]. Some panagrolaimids evolved adaptive mechanisms for rapid desiccation where most of the cellular water is lost, while others evolved freezing tolerance, without loss of water, at sub-zero temperatures by inhibiting the growth and recrystallisation of ice crystals[21]. However, the genetic and biochemical mechanisms of long term cryptobiosis in these organisms have not yet been investigated in detail.

Here we present a high-quality genome assembly and a detailed morphological, phylogenetic analysis and define a novel species, *Panagrolaimus kolymaensis.* Precise radiocarbon dating indicates that *Panagrolaimus kolymaensis* remained in cryptobiosis for about 46,000 years, since late Pleistocene. Furthermore, making use of the powerful model

organism *C. elegans*, we demonstrate that *Panagrolaimus* and *C. elegans* dauer larvae utilize similar adaptive mechanisms to survive extreme desiccation and freezing, i.e. upregulation of trehalose biosynthesis and gluconeogenesis.

Results

Discovery site and radiocarbon dating

Previously, we showed that nematodes from the Siberian permafrost with morphologies consistent with the genera *Panagrolaimus* and *Plectus* could be reanimated thousands of years after they had been frozen in the permafrost. Several viable nematode individuals were found in two out of more than 300 studied samples of permafrost deposits of different ages and genesis, collected by researchers of the Soil Cryology Lab, Pushchino, Russia, in the course of perennial paleo-ecological expeditions carried out in the coastal sector of the northeastern Arctic[17]. The detailed description of the study site (outcrop Duvanny Yar, Kolyma River, Fig.1A), sampling and revitalizing procedures are provided in Supplementary Information (SI). Like other late Pleistocene permafrost formations in the northeastern Arctic, Duvanny Yar comprises permanently frozen ice-rich silt deposits riddled with large polygonal ice wedges and divided by them into mineral blocks[26,27] (Fig.1B). The sediments include sandy alluvial layers, peat lenses, buried paleosols and Pleistocene rodent burrows (Fig.1C). The burrow (P-1320), in which *Panagrolaimus* nematodes were found (Fig.1D), has been taken from the frozen outcrop wall at a depth of about 40 m below the surface and about 11 m above river water level in undisturbed and never thawed late Pleistocene permafrost deposits. The fossil burrow left by arctic gophers of the genus *Citellus* consists of entrance tunnel and a large nesting chamber up to 25 cm in diameter[26].

The sterility of permafrost sampling and age of cultivated biota were discussed in detail in several reviews[14,28, 29]. Based on previous reports, the age of the organisms found in a burrow is equal to the freezing time and corresponds to the age of organic matter conserved in the syncryogenic sediments. This makes it possible to use radiocarbon dating of organic matter to establish the age of organisms. We performed Accelerator Mass Spectrometry (AMS) radiocarbon analysis of plant material obtained from studied borrow P-1320 and determined a direct ^{14}C age of 44,315±405 BP (Institute of Geography, RAS; sample $IGAN_{AMS}$ 9137). Calibrated age range is 45,839 – 47,769 cal BP (95.4% probability) (Fig.S1).

132 **Like other parthenogenetic *Panagrolaimus* the newly discovered species is triploid**
133 The revived animal was cultivated in the laboratory for over 100 generations and initially
134 described as *Panagrolaimus* aff. d*etritophagus*[4] based on morphology. We conducted a
135 detailed morphological analysis of the revived animal (Fig.2, S2, Table S1; see SI for details),
136 which confirmed unambiguously that the animal belongs to the genus of *Panagrolaimus*, in
137 agreement with a previous phylogenetic analysis of the 18S ribosomal RNA sequence[4].
138 However, due to the morphological uniformity of *Panagrolaimus*, unusual even for nematodes,
139 morphology and molecular analysis of a single ribosomal RNA sequence is insufficient to
140 describe a species. We found the species to be parthenogenetic, which further complicates
141 description under most species concepts.
142 To obtain comprehensive molecular data for species determination using
143 phylogenomics, we generated a genome assembly. Using PacBio HiFi sequencing, we
144 generated 84X coverage in long reads (average length 14,425 bp). Our analysis of repeat and
145 gene content is described in Supplementary Table 3. K-mer analysis of the reads clearly
146 indicated that this animal has a triploid genome (Fig.3A), similar to other parthenogenetic
147 *Panagrolaimus* species[30]. Despite the challenges that a triploid genome poses for assembly, we
148 obtained a highly-contiguous contig assembly of the three pseudohaplotypes that comprise
149 about 266 Mb and thus have a similar genome size as other parthenogenetic *Panagrolaimus*
150 species[30]. The contig N50 value of all three pseudohaplotypes is 3.8 Mb. Since the three
151 pseudohaplotypes exhibited a noticeable degree of divergence, we further investigated their
152 relationship by using the apparent homeologs in our gene predictions to align long continuous
153 contigs based on micro synteny (Fig. 3B). Links between the contigs clearly shows the triploid
154 state of the genome.
155
156 **Phylogenomics to define *Panagrolaimus kolymaensis* sp. nov.**
157 To place the species in the genus *Panagrolaimus*, we conducted a broader multi-gene
158 phylogenomic analysis using Maximum likelihood methods. Our analysis of a concatenated,
159 partitioned alignment of 60 genes, and a coalescence-based approach using a broader set of
160 12,295 gene trees, retrieves the novel species as sister to all other sequenced *Panagrolaimus*
161 species, but as an ingroup to *Propanagrolaimus*[31] (Fig.3C; Fig. S3B-C). Thus, the phylogenetic
162 placement provides strong evidence that this animal belongs to a novel species. Further
163 supporting this, there is substantial sequence divergence between this novel species, and
164 *Panagrolaimus* sp. PS1159 and *Panagrolaimus* sp. ES5, estimated to be on average 2.06 and
165 2.11 amino acid substitutions per site in our concatenated alignment, respectively. The

substantial divergence is in line with previous data on ages of *Panagrolaimus* nematodes[30], and more broadly seen in nematodes, which can be hyper-diverse[32,33]. Our data also contradicts the assumption that parthenogenesis is monophyletic trait[30] in the *Panagrolaimus* genus (Fig.3C). Based on the Kolyma River location where the animal was unearthed, we propose the following taxonomic classification and species name:

Phylum Nematoda Potts, 1932

Class Chromadorea Inglis 1983

Suborder Tylenchina Thorne, 1949

Family Panagrolaimidae Thorne, 1937

Panagrolaimus kolymaensis sp. nov.

C. elegans dauer larvae and _P. kolymaensis_ utilize similar mechanisms to enter and remain in cryptobiotic state for prolonged periods of time

In the absence of established genetic methods in *P. kolymaensis* we referred to *C. elegans* as a powerful model system to gain insights into possible pathways for long term survival[3,4,24,25]. The high-quality genome of *P. kolymaensis* allowed us to compare its molecular toolkit for cryptobiosis with that of *C. elegans*. We used orthology clustering and phylogenetics to investigate whether the genome of *P. kolymaensis* contains genes previously implicated in cryptobiosis in the *C. elegans* dauer larva. Our analysis showed that the *P. kolymaensis* genome encodes orthologs to a *C. elegans* trehalose phosphate synthase gene (*tps-2*) and to a trehalose phosphatase gene (*gob-1*) (Fig. 3D, supplementary file Orthology analysis). Furthermore, we found orthologs to all *C. elegans* enzymes required for polyamine biosynthesis, the TCA cycle, glycolysis, gluconeogenesis, and glyoxylate shunt (Fig.3D, supplementary file Orthology analysis) suggesting that *P. kolymaensis* utilizes a similar molecular tool kit as *C. elegans* to facilitate survival of unfavorable conditions.

Our earlier findings established that among several developmental stages of *C. elegans*, only the dauer larva, formed during unfavorable conditions (such as low nutrients and high population density) could survive anhydrobiosis and freezing[4,24]. To survive extreme desiccation, *C. elegans* dauer larvae need to be first preconditioned at high relative humidity (98% RH) for 4 days[24]. During preconditioning, dauer larvae upregulate trehalose biosynthesis that ensures their survival to harsh desiccation[24,25]. We tested whether preconditioning also facilitates survival of *P. kolymaensis*. Although a small proportion of *P. kolymaensis* individuals survive harsh desiccation and freezing without preconditioning (Fig.4A), mixed populations of *P. kolymaensis* survive significantly (p value< 0.0001) higher to harsh

200 desiccation upon preconditioning (Fig.4A). Similarly, preconditioning and desiccation further
201 enhanced survival rate of *P. kolymaensis* to freezing (-80°C). Like *C. elegans, P. kolymaensis*
202 upregulate trehalose levels up to 20-fold upon preconditioning (Fig.4B). We previously
203 reported that, to upregulate trehalose levels upon preconditioning, *C. elegans* dauer larva
204 dissipate their fat reserves (Triacylglycerols) by activating the glyoxylate shunt and
205 gluconeogenic pathway[25]. Upon preconditioning, we found that triacylglyceride (TAG) levels
206 are significantly decreased in *P. kolymaensis* (Fig.S5A&B). To further investigate whether the
207 acetyl-CoA derived from degradation of TAGs culminate in trehalose, we applied the
208 previously developed method of metabolic labelling with ^{14}C-acetate in combination with 2D-
209 TLC [4,25]. As shown in Fig. 4C, preconditioning led to huge increase of radioactivity in trehalose
210 and to smaller extent in some amino acids (glycine/serine, phenylalanine; panels c and d).
211 Interestingly, *P. kolymaensis* displayed an additional spot (Fig. 4D, enumerated as 7), that was
212 not found in *C. elegans*, which we identified as trehalose-6-phosphate (Fig.S5C-H), an
213 immediate precursor of trehalose, using mass spectrometry. Thus, to resist harsh desiccation,
214 like *C. elegans*, *P. kolymaensis* utilizes glyoxylate shunt and consequently acetate derived from
215 TAGs to synthesize trehalose. Detection of the immediate precursor (trehalose-6-phosphate)
216 suggests the flux of metabolites is intense in the latter.
217 Finally, we investigated whether *C. elegans* can also survive in prolonged cryptobiotic
218 state. Despite of preconditioning, the survival ability of desiccated dauer larvae at room
219 temperature declines very rapidly, with most larvae dead after around 10 days (Fig. 4E) (Fig.
220 S4A&B). Direct freezing at -80℃, leads to almost instant death of the animals. To test whether
221 combining these conditions could extend the viability of dauer larvae (Fig. S4A&B), we
222 transferred the desiccated larvae to -80℃. Remarkably, under these conditions, there was no
223 significant decline in viability even after 480 days (Fig. 4E). Moreover, after thawing, the
224 animals resumed reproductive growth and produced progeny in numbers like those of animals
225 kept under control conditions (Fig. 4F). Since no reduction in survival was observed at any
226 time point in extended experiments, these results suggest that the combination of anhydrobiosis
227 and freezing can prolong the survival ability of dauer larvae. Thus, *C. elegans*, when exposed
228 to combination of cryptobiotic states can survive for extremely long periods of time.
229
230
231
232

Discussion

Our findings here demonstrate the ability of the nematodes to survive in suspended animation for geological time scales. Along with the adaptive mechanisms of an organism, a naturally preserving ecosystem would synergistically aid the survival for prolonged periods. The Siberian permafrost is a unique repository for preserving organisms in sub-zero temperatures for millions of years. Expeditions in the past decade revived several organisms across various taxa from the Siberian permafrost[5,34,35,36]. The possibility to exploit permafrost as a source for reanimating multicellular animals was recognized already in 1936. A viable Cladocera crustacean *Chydorus sphaericus* preserved in the Transbaikalian permafrost for several thousand years[37,38] was discovered by P.N. Kapterev, who worked at the scientific station Skovorodino as a GULAG prisoner. Unfortunately, this extraordinary observation remained unnoticed for many decades.

The new species can now be placed into the genus *Panagrolaimus*[39], which contains several described and undescribed parthenogenetic and gonochoristic species and strains[30,40]. Many *Panagrolaimus* display adaptation to survival in harsh environments[21] and the genus includes the Antarctic species *P. davidii*[22]. The genus *Panagrolaimus* is exceptional in its morphological uniformity even among nematode species that are hard to classify based on morphology in general. Thus, species designation via microscopic (including SEM) analysis is unreliable, which is further complicated by the absence of males in parthenogenetic species makes. Males have important diagnostic features as spicules and pericloacal papillae, females differ from one species to another mainly by morphometrics, whereby the interspecies differences (absolute measures and ratios) may be very fine. Our specimens are close by absolute sizes and ratios to females of the bisexual species *Panagrolaimus detritophagus*[41]. The only non- overlapping morphometric character is index “b” (body length: pharynx length): 5.6–6.8 in *P. kolymaensis* versus 4.4-5.1 in *P. detritophagus*.

Consequently, we turned to phylogenomics methods to place the species on the tree. This showed that species is an outgroup to other known *Panagrolaimus* species, raising for the possibility of a second independent evolution of parthenogenesis in the genus, in contrast to previous findings[40,31,30]. This will need to be confirmed through further sampling and genome sequencing of *Panagrolaimus* species. We found *P. kolymaensis* to be triploid and thus a hybrid origin is possible, as seen in other parthenogenetic *Pangrolaimus*[30]. The highly contiguous genome of *P. kolymaensis* will allow for analyses of this trait in comparison to other *Panagrolaimus* species currently being genome sequenced. The successful phylogenomic

species identification we conducted here demonstrates the utility of this method for morphologically hard to identify species, in particular when the additional data yielded by a fully sequenced genome are considered.

Our results provide a deeper insight into the homology of molecular and biochemical mechanisms between *C. elegans* and *P. kolymaensis*, which are not only taxonomically but also ecologically distinct. *C. elegans* can mostly be found in rotting fruits and plants in temperate regions[42,43], while *Panagrolaimus* species are globally distributed and prevalent in leaf litter and soil[40], including in harsh environments[21]. We show through orthology analysis that the well-studied molecular pathways used by *C. elegans* larvae to enter the dauer state, such as insulin[44,45] (DAF-11, DAF-2 & DAF-16), TGF-β[46] (DAF-7), steroid[47] (DAF-9, DAF-12) are present in the genome of the *P. kolymaensis* (Fig.S4C). While further functional analyses are needed to study molecular pathways detail, our results hint at convergence or parallelism in the molecular mechanisms organizing dauer formation and cryptobiosis.

As mentioned earlier preconditioning enhances the survival of *P. kolymaensis* to desiccation and freezing. We previously reported that preconditioning induces trehalose upregulation in *C. elegans* dauer larvae and the elevated trehalose renders desiccation tolerance by protecting the cellular membranes[24]. It is not surprising that *P. kolymaensis* upregulates trehalose, however the magnitude of trehalose elevation is higher than *C. elegans* dauer larvae. This indicates that central regulators (DAF-16, DAF-12) of trehalose upregulation may differentially regulate *tps-2* in *P. kolymaensis*[48,49]. Although *P. kolymaensis* utilizes glyoxylate shunt and gluconeogenesis to upregulate trehalose levels, it is intriguing to observe that they accumulate substantial levels of trehalose-6-phosphate. Further investigation of this observation using perturbation experiments will provide insights into metabolic regulation in *P. kolymaensis* upon preconditioning. Our findings for the first time demonstrate that *C. elegans* dauer larvae possess an inherent ability to survive freezing for prolonged periods if they undergo anhydrobiosis. It is tempting to speculate that undergoing anhydrobiosis might be a survival strategy of *C. elegans* to survives seasonal changes in nature.

In summary our findings indicate that by adapting to survive cryptobiotic state for short time frames in environments like permafrost, some nematode species gained the potential for individual worms to remain in the state for geological timeframes. This raises the question whether there is an upper limit to the length of time an individual can remain in the cryptobiotic state, potentially only limited by drastic changes to the environment such as strong fluctuations in ambient temperature, natural radioactivity, or other abiotic factors. These findings have

implications for our understanding of evolutionary processes, since generation times could be stretched from days to millennia, species ages might be much longer than anticipated, and long-term survival of individuals of species can lead to the refoundation of otherwise extinct lineages. Finally, understanding the precise mechanisms of long-term cryptobiosis and cues that lead to successful revivals can inform new methods for long term storage of cells and tissues.

305 **Methods:**

306 **Materials and *C. elegans* strains**

307 [1-14C] -acetate (sodium salt) from Hartmann Analytic (Braunschweig, Germany). All other
308 chemicals were purchased from Sigma-Aldrich (Taufkirchen, Germany). The *Caenorhabditis*
309 Genetic Centre (CGC) provided *daf-2(e1370)* and *E. coli NA22* strains.

310

311 **Genomic DNA isolation from *Panagrolaimus kolymaensis* nematodes**

312 *P. kolymaensis* nematodes were grown on several plates of NGM agar plated with *E. Coli NA22*
313 bacteria at 20°C. Worms were collected from the plates, washed with water at least three to
314 five times by centrifugation at 1000 g to remove any residual bacteria and any debris. The
315 worm pellet was dissolved in 5 volumes of worm lysis buffer (0.1M Tris-HCl pH=8.5, 0.1M
316 NaCl, 50mM EDTA pH=8.0) and distributed in 1.5 ml of microcentrifuge tubes. These tubes
317 are incubated at -80°C for 20 minutes. 100 µl of Proteinase 'K' (20 mg/ml) was added to each
318 tube and they are incubated at 60°C overnight. 625 µl of cold GTC buffer (4M Guanidinium
319 Thiocynate, 25mM Sodium citrate, 0.5% (v\v) N-lauroylsarcosine, 7%(v/v) Beta
320 Mercaptoethanol) was added to the tube, incubated on ice 30 min, and mixed by inverting every
321 10 min. 1 volume of phenol–chloroform-isoamyl alcohol (pH=8) was added to the lysate and
322 mixed by inverting the tube 10-15 times. Tubes were centrifuged for 5 min at 10,000 g at 4 °C
323 to separate the phases. The upper aqueous phase was carefully collected into a fresh tube. One
324 volume of fresh chloroform was added and mixed by inverting the tubes for 10-15 times and
325 centrifuged for 5 min at 10,000 g at 4°C to separate the phases. One volume of cold 5 M NaCl
326 was added, mixed by inverting the tubes and incubated on ice for 15 min. After incubation
327 these tubes were centrifuged for 15 min at 12,000–16,000 g at 4 °C. The supernatant containing
328 the nucleic acids were slowly transferred into a fresh tube. One volume of isopropanol was
329 added to the tube, inverted few times, and incubated on ice for 30 minutes. After incubation,
330 the tubes were centrifuged at 3000 g for 30–45 min at 25°C and the supernatant was discarded
331 without disturbing the pellet. The pellet was washed twice with 1 ml of 70% ethanol, tubes
332 were centrifuged at 3000 g for 5 min and supernatant was discarded and incubated at 37°C for
333 10-15 min to dry the pellet. The pellet was resuspended carefully in TE buffer. The quality of
334 the genomic DNA was analyzed with pulse field gel electrophoresis.

335

336

337

338 **Genome sequencing and assembly**

339 Long insert library has been prepared as recommended by Pacific Bioscienes according to
340 theprotocol 'Procedure & Checklist-Preparing gDNA Libraries Using the SMRTbell® Express
341 Template Preparation Kit 2.0'. In summary, RNAse treated HMW gDNA has been sheared to
342 20Kb fragments on the MegaRuptor™ device (Diagenode) and 10 µg sheared gDNA have
343 been used for library preparation. The PacBio SMRTbell™ library was size selected in two
344 fractions (9-13kb, > 13kb) using the BluePippin™ device with cassette definition of 0.75% DF
345 MarkerS1 3-10 kb Improved Recovery. The second fraction of the size selected library has
346 been loaded with 95 pM on plate on a Sequel SMRT cell (8M). Sequel polymerase 2.0 has
347 been used in combination with the v2 PacBio sequencing primer and the Sequel sequencing kit
348 2.0EA, runtime was 30 hours. We created PacBio CCS reads from the subreads.bam file using
349 PacBio's ccs command linetool (version4.2.0). We obtained 8.5Gb hiqh quality CCS reads
350 (HiFi reads) with a N50 of 14.4 Kb. We ran HiCanu (version 2.2)[39] to create the contig
351 assembly. Blobtools (version 1.1.1,CITE:) was used to identify and remove bacterial contigs.
352 The final triploid contig assembly consists of 856 contigs has a N50 of 3.82 Mb and a size of
353 266Mb. The mitochondrial genome was created with the mitoHifi pipeline (version
354 2, https://github.com/marcelauliano/MitoHiFi) based on the assembled contigs and the closely
355 related reference mitochondrial genome of Panagrellus redivivus (strain: PS2298/MT8872,
356 ENAaccession: AP017464). The mitoHifi pipeline identified 49 mitochondrial contigs ranging
357 from 13-32Kb. The final annotated circular mitochondrial genome has length of 17467 bp.
358 To identify pseudohaplotypes in the *P. kolymanensis* sp. nov genome assembly, we selected
359 the longest isoform of each predicted protein-coding gene in our assembly and in the *C. elegans*
360 genome (downloaded from WormBase Parasite, release WBPS15) using AGAT (version 0.4.0)
361 and clustered them into orthologous groups (OGs) using OrthoFinder (version 2.5.2). We
362 identified OGs that contained three *Panagrolaimus* sequences (i.e. groups that were present as
363 single-copy in all three pseudohaplotypes) and used these to identify trios of multi-megabase
364 size contigs derived from the three pseudohaplotypes. We visualized synteny between the three
365 pseudohaplotypes using Circos to plot the positions of each homeolog (version 0.69-8).
366

367 **Genome annotation**

368 We used RepeatModeler 1.0.8 (http://www.repeatmasker.org/) with parameter '-engine ncbi'
369 to create a library of repeat families. This library was used with RepeatMasker 4.0.9 to soft-
370 mask the *Panagrolaimus* genome. To annotate genes, we cross mapped protein models from

371 an existing *Panagrolaimus* as external evidence in the Augustus[51] based pipeline. We evaluated
372 the completeness of our predictions using BUSCO on the gVolante web interface.
373
374 **Orthology analysis**
375 We conducted a gene orthology analysis using genomic data from *Panagrolaimus kolymaensis*,
376 the plectid nematode species from the permafrost, as well as genomic data from WormBase
377 Parasite (https://parasite.wormbase.org; accessed 17/12/2020): *Caenorhabditis elegans*,
378 *Diploscapter coronatus*, *Diploscapter pachys*, *Halicephalobus mephisto*, *Panagrellus*
379 *redivivus*, *Panagrolaimus davidi*, *Panagrolaimus* sp. ES5, *Panagrolaimus* sp. PS1159,
380 *Panagrolaimus superbus*, *Plectus sambesii*, and *Propanagrolaimus* sp. JU765. For plectids,
381 genomic resources are scarce. We therefore added transcriptome data of *Plectus murrayi*,
382 *Anaplectus granulosus*, *Neocamacolaimus parasiticus*, and *Stephanolaimus elegans*. The latter
383 three transcriptomes were kindly provided by Dr. Oleksandr Holovachov (Swedish museum of
384 natural history). The *Anaplectus granulosus*, and *Neocamacolaimus parasiticus* transcriptomes
385 have been published [52,53]. All three transcriptomes were assembled de novo with Trinity[54]. The
386 exact procedures are described in the respective publications[52,53] . The *Stephanolaimus* elegans
387 transcriptome was assembled in the same way as described for *Neocamacolaimus parasiticus*.
388 The *Plectus murrayi* transcriptome was built from raw reads deposited at NCBI (https://sra-
389 downloadb.be-md.ncbi.nlm.nih.gov/sos2/sra-pub-run-13/SRR6827978/SRR6827978.1;
390 accessed 22.12.2020). The transcriptome was assembled using Galaxy Trinity version 2.9.1[55],
391 [54] using all default options and including in silico normalization of reads before assembly.
392 Transdecoder (conda version 5.5.0)[56] was used to translate to amino acid sequence. Identical
393 reads were removed with cd-hit version 4.8.1[57,58], and the Trinity
394 get_longest_isoform_seq_per_trinity_gene.pl command[56] (Trinity conda version 2.8.5)
395 {Anaconda Software Distribution, Conda, Version 4.9.2, Anaconda, Nov. 2020; was used, to
396 remove shorter isoforms. Amino acid translated longest isoforms from genomic data were
397 extracted with AGAT {Dainat, https://www.doi.org/10.5281/zenodo.3552717} from genome
398 assembly FASTA files and genome annotation GFF3 files, using the
399 agat_convert_sp_gxf2gxf.pl command to convert all GFF3 files to the required GFF3 format,
400 and the agat_sp_keep_longest_isoform.pl as well as the agat_sp_extract_sequences.pl
401 commands to extract amino acid translated FASTA files. The headers and names of all FASTA
402 files were modified to allow for simple species assignment of each sequence in subsequent
403 analysis. The orthology analysis was conducted with OrthoFinder v. 2.5.1[59,60] using default
404 settings. For genes of interest, we constructed alignments with MAFFT v. 7.475[61] using the

405 localpair and maxiterate (1000) functions. We removed spurious sequences and areas that were
406 not well aligned with Trimal v. 1.4.rev22[62] (procedure stated in supplementary file Orthology
407 analysis below each phylogeny). We then ran phylogenetic analysis with Iqtree2 v. 2.0.6[63],
408 with -bb 1000 option, testing the model for each analysis (models eventually used stated in
409 supplementary file Orthology analysis). We also checked for PFAM domains using
410 Interproscan v. 5.50-84.0[64]. Part of the analysis was performed on the HPC RRZK CHEOPS
411 of the Regional Computing Centre (RRZK) of the University of Cologne. The phylogenies
412 were visualized with Dendroscope 3.7.6[65] and figures were created with Inkscape
413 {https://inkscape.org}.
414
415 **Phylogenomics**
416 Sequences of 18S and 28S genes from 44 taxa across the *Propanagrolaimus*, *Panagrolaimus*,
417 *Panagrellus* and *Halicephalobus* genera were aligned (MAFFT L-INS-I v7.475)[61],
418 concatenated [66]and used to infer a species tree using maximum likelihood via (IQTREE)[67] and
419 partitioned by best-fit models of sequence evolution for both[68]. Nodal support was determined
420 using 1000 bootstrap pseudoreplicates. A further 60 genes from 101 taxa were used to confirm
421 the taxonomic position using the supermatrix concatenation methods outlined above. Given the
422 limitations of differential gene sampling, we expanded our phylogenomic analyses to include
423 a coalescence approach using 12,295 ML gene trees inferred for orthogroups containing the
424 target animal. Instances of multiple genes per species per group were treated as
425 paralogs/orthologs and analysed using ASTRAL-Pro[69].
426
427 **Desiccation survival assay**
428 *C. elegans* dauer larvae desiccation assays were performed as described in. *Panagrolaimus*
429 *kolymaensis* desiccation assays were performed with mixed populations of the worms.
430
431 **Exposure of nematodes to extreme environments**
432 Dauer larvae or *Panagrolaimus kolymaensis* nematodes were preconditioned and desiccated as
433 described[24] and then transferred to elevated temperature of 34°C, freezing (-80°C) and anoxia.
434 Anoxic environment was generated in a desiccation chamber at 60%RH by flushing the
435 Nitrogen gas into the chamber. The concentration of oxygen inside the chamber was monitored.
436 After each timepoint they were rehydrated with 500 µl of water for 2-3 hours. Rehydrated
437 worms were transferred to NGM agar plates with *E. Coli NA22* as food. Survivors were counted

438 after overnight recovery. Each experiment was performed on two different days with at least
439 two technical replicates.
440
441 **Trehalose quantification from nematode lysates**
442 Trehalose measurements were performed as described in previous reports[25].
443
444 **Radiolabeling, metabolite extraction and 2D-TLC**
445 The above-mentioned procedures were performed according to previous reports[3,25].

446 **Identification of trehalose-6-phosphate from TLC plates**
447 Normalised aqueous fractions from the non-preconditioned and preconditioned samples were
448 separated by high performance thin layer chromatography (HPTLC), using 1-propanol-
449 methanol-ammonia (32%)-water (28:8:7:7 v/v/v/v) as first, dried for 15 min and 1-butanol-
450 acetone-glacial acetic acid–water (35:35:7:23 v/v/v/v) second dimension respectively. Using
451 the trehalose as a standard on both dimensions of the TLC, the regions of interest were scrapped
452 out from the TLCs. The scraped-out silica was extracted with 10 ml of 50% methanol twice.
453 The fractions were combined, dried under vacuum and dissolved in 100 µl of Ms mix solution
454 containing 4:2:1 (Isopropanol:Methanol:Chloroform) with 7.5 mM ammonium formate. Mass
455 spectrometric analysis was performed on a Q Exactive instrument (Thermo Fischer Scientific,
456 Bremen, DE) equipped with a robotic nanoflow ion source TriVersa NanoMate (Advion
457 BioSciences, Ithaca, USA) using nanoelectrospray chips with a diameter of 4.1 µm. The ion
458 source was controlled by the Chipsoft 8.3.1 software (Advion BioSciences). Ionization voltage
459 was + 0.96 kV in negative mode; backpressure was set at 1.25 psi. The temperature of the ion
460 transfer capillary was 200°C; S-lens RF level was set to 50%. FT MS spectra were acquired
461 within the range of m/z 50–750 at the mass resolution of R m/z 200 = 140000; automated gain
462 control (AGC) of 3×10^6 and with the maximal injection time of 3000 ms. FT MS/MS spectra
463 were acquired within the range of m/z 50–750 at the mass resolution of R m/z 200 = 140000;
464 automated gain control (AGC) of 3×10^4 and with the maximal injection time of 30 s.
465
466 **Triacylglycerols measurement from *Panagrolaimus kolymaensis* lysates**
467 Non-preconditioned and preconditioned pellets were lysed in 200 µl of isopropanol with 0.5
468 mm Zirconium beads twice for 15 min. The lysates were centrifuged at 1300 g for 5 min. The
469 supernatant was carefully collected without any debris, 20 µl of the lysate was used for protein
470 estimation. Normalization was performed according to soluble protein levels, supernatant

471 volumes corresponding to 50-100 µg of proteins were dried in the desiccator. 700 µl of IS
472 ((10:3 (Methyl tert-butyl ether: ethanol)) mix (warmed to room temperature) was added to
473 dried samples and left on a shaker for 1 hour. The samples were centrifuged at 1400 rpm and
474 4°C. 140 µl of water was added and left on shaker for 15 min. These samples were centrifuged
475 at 13400 rpm for 15 min. The upper organic fraction was collected and transferred to 1.5 ml
476 glass vial and left for drying in the desiccator. The dried samples were reconstituted in
477 appropriate volume of 300 µl of 4:2:1 (Isopropanol:Methanol:Chloroform) and volume
478 corresponding 1 µg was used for injection.
479 LC-MS/MS analysis was performed on a high-performance liquid chromatography
480 system (Agilent 1200 HPLC) coupled to a Xevo G2-S QTof (Waters). The samples were
481 resolved on a reverse phase C18 column (Cortecs C18 2.7um from Waters) with 50:50:0.1:1%
482 (Water:methanol:formic acid: 1M Ammonium formate) and 25:85:0.1:1%
483 (Acetonitrile:Isopropanol:Formic acid:1M Ammonium formate) as mobile phase. The
484 following gradient program was used: Eluent B from 0 % to 100 % within 12 min; 100 % from
485 12 min to 17min; 0 % from 17 min to 25 min. The flow rate was set at 0.3 ml/min. The samples
486 were normalised according to the total protein concentration and the worm numbers. TGD
487 50:00:00 was used as internal standard. Skyline software was used to analyse the raw data. The
488 TG were extracted from Lipidmaps database.
489
490
491
492
493
494
495
496
497
498
499
500
501
502
503
504

505 **Author contributions**

506 AS, VG, PS, TK conceived and designed the study. AS, VG, TH, MP, AT, GH, MH, ER, PS
507 and TK contributed to the original draft. AS performed isolation and cultivation of nematodes.
508 VG performed desiccation survival assays, trehalose measurement, 2D-TLC of metabolites,
509 trehalose-6-phosphate detection, combination of cryptobiosis experiments, genomic DNA
510 isolation from *Panagrolaimus kolymaensis*, assembled the data from all the authors and
511 prepared the figures. MP performed genome assembly. TH conducted orthology analyses and
512 single gene phylogenies and worked on figures. AT provided morphological description, light,
513 and scanning electron microscopy. LS analyzed the genome assembly and created figures.
514 GMH performed the phylogenetic analyses. ST performed triacylglycerols measurements,
515 trehalose-6-phosphate detection with suggestions from Andrej Shevchenko. MH annotated
516 supplementary table 3. PS performed genome annotation and supervised TH and LS. EWM
517 supervised MP and had overall responsibility for sequencing and assembly including funding
518 it.
519
520
521
522
523
524
525
526
527
528
529
530
531
532
533
534
535
536
537

Acknowledgements

VG is thankful to Andrej Shevchenko, members of Kurzchalia lab for helpful discussions and core facilities of MPI-CBG for assistance. We are grateful to Dr. S. Gubin for field study and sampling, our colleagues in Soil Cryology Lab, Pushchino and North-East Scientific Station in Chersky, Republic of Sakha (Yakutia) for their help and cooperation. The authors thank Long Read Team of the DRESDEN-concept Genome Center, DFG NGS Competence Center, part of the Center for Molecular and Cellular Bioengineering (CMCB), Technische Universität Dresden and MPI-CBG. GMH is funded by a UCD Ad Astra Fellowship. This work was supported by the Russian Foundation for Basic Research (19-29-05003-mk) to AS and ER. VG and TK financial support from the Volkswagen Foundation (Life? research grant 92847). PS and TH are supported by a DFG ENP grant to PS (DFG project 434028868). The authors are thankful to Richard Roy and Jens Bast for critical reading the manuscript. We thank Iain Pattern for suggestions in writing the manuscript.

References

1. Hibshman, J. D., Clegg, J. S. & Goldstein, B. Mechanisms of Desiccation Tolerance: Themes and Variations in Brine Shrimp, Roundworms, and Tardigrades. *Front. Physiol.* **11**, 592016 (2020).
2. Erkut, C. *et al.* Molecular Strategies of the Caenorhabditis elegans Dauer Larva to Survive Extreme Desiccation. *PLoS ONE* **8**, e82473 (2013).
3. Gade, V. R., Traikov, S., Oertel, J., Fahmy, K. & Kurzchalia, T. V. C. elegans possess a general program to enter cryptobiosis that allows dauer larvae to survive different kinds of abiotic stress. *Sci. Rep.* **10**, 13466 (2020).
4. Shatilovich, A. V. *et al.* Viable Nematodes from Late Pleistocene Permafrost of the Kolyma River Lowland. *Dokl. Biol. Sci.* **480**, 100–102 (2018).
5. Shmakova, L. *et al.* A living bdelloid rotifer from 24,000-year-old Arctic permafrost. *Curr. Biol.* **31**, R712–R713 (2021).
6. Keilin, D. The Leeuwenhoek Lecture - The problem of anabiosis or latent life: history and current concept. *Proc. R. Soc. Lond. Ser. B - Biol. Sci.* **150**, 149–191 (1959).
7. Cano, R. & Borucki, M. Revival and identification of bacterial spores in 25- to 40-million-year-old Dominican amber. *Science* **268**, 1060–1064 (1995).
8. Shen-Miller, J. Sacred lotus, the long-living fruits of China Antique. *Seed Sci. Res.* **12**, 131–143 (2002).
9. Guidetti, R. & Jönsson, K. I. Long-term anhydrobiotic survival in semi-terrestrial micrometazoans. *J. Zool.* **257**, 181–187 (2002).
10. Tsujimoto, M., Imura, S. & Kanda, H. Recovery and reproduction of an Antarctic tardigrade retrieved from a moss sample frozen for over 30 years. *Cryobiology* **72**, 78–81 (2016).
11. Kagoshima, H. *et al.* Multi-decadal survival of an Antarctic nematode, Plectus murrayi, in a -20°C stored moss sample. 9.
12. Aroian, R. V., Carta, L., Kaloshian, I. & Sternberg, P. W. A Free - living Panagrolaimus sp. from Armenia Can Survive in Anhydrobiosis for 8.7 Years. 3.
13. Gilichinsky, D. A. *et al.* Microbial Populations in Antarctic Permafrost: Biodiversity, State, Age, and Implication for Astrobiology. *Astrobiology* **7**, 275–311 (2007).
14. Rivkina, E. *et al.* Earth's perennially frozen environments as a model of cryogenic planet ecosystems. *Permafr. Periglac. Process.* **29**, 246–256 (2018).

15. Sipes, K. *et al.* Eight Metagenome-Assembled Genomes Provide Evidence for Microbial Adaptation in 20,000- to 1,000,000-Year-Old Siberian Permafrost. *Appl. Environ. Microbiol.* **87**, (2021).
16. Liang, R. *et al.* Genomic reconstruction of fossil and living microorganisms in ancient Siberian permafrost. *Microbiome* **9**, 110 (2021).
17. Gilichinsky, D. A. & Rivkina, E. M. Permafrost microbiology. 7 (2011).
18. Yashina, S. *et al.* Regeneration of whole fertile plants from 30,000-y-old fruit tissue buried in Siberian permafrost. *Proc. Natl. Acad. Sci.* **109**, 4008–4013 (2012).
19. Adhikari, B. N., Wall, D. H. & Adams, B. J. Desiccation survival in an Antarctic nematode: molecular analysis using expressed sequenced tags. *BMC Genomics* **10**, 69 (2009).
20. Tyson, T. *et al.* A molecular analysis of desiccation tolerance mechanisms in the anhydrobiotic nematode Panagrolaimus superbus using expressed sequenced tags. *BMC Res. Notes* **5**, 68 (2012).
21. McGill, L. M. *et al.* Anhydrobiosis and Freezing-Tolerance: Adaptations That Facilitate the Establishment of Panagrolaimus Nematodes in Polar Habitats. *PLOS ONE* **10**, e0116084 (2015).
22. Thorne, M. A. S., Kagoshima, H., Clark, M. S., Marshall, C. J. & Wharton, D. A. Molecular Analysis of the Cold Tolerant Antarctic Nematode, Panagrolaimus davidi. *PLoS ONE* **9**, e104526 (2014).
23. Sandhove, J., Spann, N. & Ristau, K. The Anhydrobiotic Potential of the Terrestrial Nematodes *Plectus parietinus* and *Plectus velox*: Anhydrobiosis of *plectus parietinus* and *p. velox*. *J. Exp. Zool. Part Ecol. Genet. Physiol.* **325**, 434–440 (2016).
24. Erkut, C. *et al.* Trehalose Renders the Dauer Larva of Caenorhabditis elegans Resistant to Extreme Desiccation. *Curr. Biol.* **21**, 1331–1336 (2011).
25. Erkut, C., Gade, V. R., Laxman, S. & Kurzchalia, T. V. The glyoxylate shunt is essential for desiccation tolerance in C. elegans and budding yeast. *elife* **5**, (2016).
26. Zanina, O. G., Gubin, S. V., Kuzmina, S. A., Maximovich, S. V. & Lopatina, D. A. Late-Pleistocene (MIS 3-2) palaeoenvironments as recorded by sediments, palaeosols, and ground-squirrel nests at Duvanny Yar, Kolyma lowland, northeast Siberia. *Quat. Sci. Rev.* **30**, 2107–2123 (2011).
27. Murton, J. B. *et al.* Palaeoenvironmental Interpretation of Yedoma Silt (Ice Complex) Deposition as Cold-Climate Loess, Duvanny Yar, Northeast Siberia: Palaeoenvironmental Interpretation of Yedoma Silt, Duvanny Yar. *Permafr. Periglac. Process.* **26**, 208–288 (2015).

634 28.Abramov, A., Vishnivetskaya, T. & Rivkina, E. Are permafrost microorganisms as old as
635 permafrost? *FEMS Microbiol. Ecol.* **97**, fiaa260 (2021).
636 29.Gilichinsky, D. A., Wagener, S. & Vishnevetskaya, T. A. Permafrost microbiology.
637 *Permafr. Periglac. Process.* **6**, 281–291 (1995).
638 30.Schiffer, P. H. *et al.* Signatures of the Evolution of Parthenogenesis and Cryptobiosis in the
639 Genomes of Panagrolaimid Nematodes. *iScience* **21**, 587–602 (2019).
640 31.Schiffer, P. H. *et al.* Developmental variations among Panagrolaimid nematodes indicate
641 developmental system drift within a small taxonomic unit. *Dev. Genes Evol.* **224**, 183–188
642 (2014).
643 32.Dey, A., Chan, C. K. W., Thomas, C. G. & Cutter, A. D. Molecular hyperdiversity defines
644 populations of the nematode Caenorhabditis brenneri. *Proc. Natl. Acad. Sci.* **110**, 11056–
645 11060 (2013).
646 33.Cutter, A. D. Divergence Times in Caenorhabditis and Drosophila Inferred from Direct
647 Estimates of the Neutral Mutation Rate. *Mol. Biol. Evol.* **25**, 778–786 (2008).
648 34.Malavin, S., Shmakova, L., Claverie, J.-M. & Rivkina, E. Frozen Zoo: a collection of
649 permafrost samples containing viable protists and their viruses. *Biodivers. Data J.* **8**, e51586
650 (2020).
651 35.Krivushin, K. *et al.* Two Metagenomes from Late Pleistocene Northeast Siberian
652 Permafrost. *Genome Announc.* **3**, e01380-14 (2015).
653 36.Zhou, J. *et al.* Phylogenetic diversity of a bacterial community determined from Siberian
654 tundra soil DNA. *Microbiology* **143**, 3913–3919 (1997).
655 37.Kapterev, P. Anabiosis in the conditions of permanent congelation. *Izv Akad Nauk SSSR Ser*
656 *Biol* **6**, 1073–1088 (1936).
657 38.Kapterev, P. New data on revitalization of organisms from perpetually frozen grounds. *CR*
658 *Acad Sci URSS* **20**, 315–317 (1938).
659 39.Andrássy, I. *Klasse Nematoda*. (Gustav Fischer Verlag, 1984).
660 40.Lewis, S. C. *et al.* Molecular evolution in Panagrolaimus nematodes: origins of
661 parthenogenesis, hermaphroditism and the Antarctic species P. davidi. *BMC Evol. Biol.* **9**,
662 15 (2009).
663 41.Andrássy, I. *Free-living Nematodes of Hungary*. (Hungarian Natural History Museum,
664 2005).
665 42.Schulenburg, H. & Félix, M.-A. The Natural Biotic Environment of *Caenorhabditis elegans*.
666 *Genetics* **206**, 55–86 (2017).
667 43.Frézal, L. & Félix, M.-A. C. elegans outside the Petri dish. *eLife* **4**, e05849 (2015).

668 44.Gems, D. *et al.* Two pleiotropic classes of daf-2 mutation affect larval arrest, adult behavior,
669 reproduction and longevity in Caenorhabditis elegans. *Genetics* **150**, 129–155 (1998).
670 45.Vowels, J. J. & Thomas, J. H. Multiple chemosensory defects in daf-11 and daf-21 mutants
671 of Caenorhabditis elegans. *Genetics* **138**, 303–316 (1994).
672 46.Ren Peifeng *et al.* Control of C. elegans Larval Development by Neuronal Expression of a
673 TGF-β Homolog. *Science* **274**, 1389–1391 (1996).
674 47.Gerisch, B., Weitzel, C., Kober-Eisermann, C., Rottiers, V. & Antebi, A. A Hormonal
675 Signaling Pathway Influencing C. elegans Metabolism, Reproductive Development, and
676 Life Span. *Dev. Cell* **1**, 841–851 (2001).
677 48.Penkov, S. *et al.* Integration of carbohydrate metabolism and redox state controls dauer
678 larva formation in Caenorhabditis elegans. *Nat. Commun.* **6**, 8060 (2015).
679 49.Penkov, S. *et al.* A metabolic switch regulates the transition between growth and diapause
680 in C. elegans. *BMC Biol.* **18**, 31 (2020).
681 50.Nurk, S. *et al.* HiCanu: accurate assembly of segmental duplications, satellites, and allelic
682 variants from high-fidelity long reads. *Genome Res.* **30**, 1291–1305 (2020).
683 51.Brůna, T., Hoff, K. J., Lomsadze, A., Stanke, M. & Borodovsky, M. BRAKER2: automatic
684 eukaryotic genome annotation with GeneMark-EP+ and AUGUSTUS supported by a
685 protein database. *NAR Genomics Bioinforma.* **3**, lqaa108 (2021).
686 52.Smythe, A. B., Holovachov, O. & Kocot, K. M. Improved phylogenomic sampling of free-
687 living nematodes enhances resolution of higher-level nematode phylogeny. *BMC Evol. Biol.*
688 **19**, 121 (2019).
689 53.Ahmed, M., Adedidran, F. & Holovachov, O. A draft transcriptome of a parasite
690 Neocamacolaimus parasiticus (Camacolaimidae, Plectida). *J. Nematol.* **53**, 1–4 (2021).
691 54.Grabherr, M. G. *et al.* Full-length transcriptome assembly from RNA-Seq data without a
692 reference genome. *Nat. Biotechnol.* **29**, 644–652 (2011).
693 55.Goecks, J., Nekrutenko, A., Taylor, J. & Galaxy Team, T. Galaxy: a comprehensive
694 approach for supporting accessible, reproducible, and transparent computational research in
695 the life sciences. *Genome Biol.* **11**, R86 (2010).
696 56.Haas, B. J. *et al.* De novo transcript sequence reconstruction from RNA-seq using the
697 Trinity platform for reference generation and analysis. *Nat. Protoc.* **8**, 1494–1512 (2013).
698 57.Li, W. & Godzik, A. Cd-hit: a fast program for clustering and comparing large sets of
699 protein or nucleotide sequences. *Bioinformatics* **22**, 1658–1659 (2006).
700 58.Fu, L., Niu, B., Zhu, Z., Wu, S. & Li, W. CD-HIT: accelerated for clustering the next-
701 generation sequencing data. *Bioinformatics* **28**, 3150–3152 (2012).

59. Emms, D. M. & Kelly, S. OrthoFinder: solving fundamental biases in whole genome comparisons dramatically improves orthogroup inference accuracy. *Genome Biol.* **16**, 157 (2015).
60. Emms, D. M. & Kelly, S. OrthoFinder: phylogenetic orthology inference for comparative genomics. *Genome Biol.* **20**, 238 (2019).
61. Katoh, K. & Standley, D. M. MAFFT Multiple Sequence Alignment Software Version 7: Improvements in Performance and Usability. *Mol. Biol. Evol.* **30**, 772–780 (2013).
62. Capella-Gutierrez, S., Silla-Martinez, J. M. & Gabaldon, T. trimAl: a tool for automated alignment trimming in large-scale phylogenetic analyses. *Bioinformatics* **25**, 1972–1973 (2009).
63. Minh, B. Q. *et al.* IQ-TREE 2: New Models and Efficient Methods for Phylogenetic Inference in the Genomic Era. *Mol. Biol. Evol.* **37**, 1530–1534 (2020).
64. Jones, P. *et al.* InterProScan 5: genome-scale protein function classification. *Bioinformatics* **30**, 1236–1240 (2014).
65. Huson, D. H. & Scornavacca, C. Dendroscope 3: An Interactive Tool for Rooted Phylogenetic Trees and Networks. *Syst. Biol.* **61**, 1061–1067 (2012).
66. Kück, P. & Meusemann, K. FASconCAT: Convenient handling of data matrices. *Mol. Phylogenet. Evol.* **56**, 1115–1118 (2010).
67. Nguyen, L.-T., Schmidt, H. A., von Haeseler, A. & Minh, B. Q. IQ-TREE: A Fast and Effective Stochastic Algorithm for Estimating Maximum-Likelihood Phylogenies. *Mol. Biol. Evol.* **32**, 268–274 (2015).
68. Kalyaanamoorthy, S., Minh, B. Q., Wong, T. K. F., von Haeseler, A. & Jermiin, L. S. ModelFinder: fast model selection for accurate phylogenetic estimates. *Nat. Methods* **14**, 587–589 (2017).
69. Zhang, C., Scornavacca, C., Molloy, E. K. & Mirarab, S. ASTRAL-Pro: Quartet-Based Species-Tree Inference despite Paralogy. *Mol. Biol. Evol.* **37**, 3292–3307 (2020).
70. Ranallo-Benavidez, T. R., Jaron, K. S. & Schatz, M. C. GenomeScope 2.0 and Smudgeplot for reference-free profiling of polyploid genomes. *Nat. Commun.* **11**, 1432 (2020).
71. Kokot, M., Długosz, M. & Deorowicz, S. KMC 3: counting and manipulating k-mer statistics. *Bioinformatics* **33**, 2759–2761 (2017).

Figure legends

Figure 1. Study site.

a) location of the Duvanny Yar outcrope on the Kolyma River, northeastern Siberia, Russia. b) view of the upper part of outcrop composed of ice wedges and permafrost silty deposits. c) lithostratigraphic scheme of deposits, showing location of studied rodent borrow (red circle). d) fossil rodent burrow with herbaceous litter and seeds buried in permafrost deposits; m a.r.l. = meters above river level.

Figure 2. General morphology of *Panagrolaimus kolymaensis* sp. n., female.

Scanning electron pictures (a, c), light microscopy photographs (e, f) and graphic presentations (b, d, g) of holotype: a, b) entire body, c, d) anterior ends, e) anterior body, f) perivulvar body region, g) tail. Abbreviations: l.f. – lateral field, ov – ovary, pro – procorpus of the pharynx, t.b. – terminal bulb of the pharynx, u – uterus with eggs, v – vulva, v.p. – ventral pore. Scale bars: a, d, e, f, g – 20 µm, b – 100 µm, c – 2 µm.

802 **Figure 3. Genome assembly and phylogenomics reveals that the newly discovered**
803 ***Panagrolaimus kolymaensis* species is triploid.**
804 a) Kmer spectra of the *Panagrolaimus kolymaensis* PacBio HiFi data. Kmers of length 19 were
805 counted using Jellyfish. b) Circos plot showing the triploid structure of the *Panagrolaimus*
806 *kolymensis* genome. The relationship between eight contigs, representing 39.9 Mb (15%) of
807 the genome, is shown. Numbers represent the contig IDs. c) Inferred species tree for all taxa.
808 The maximum likelihood tree inferred using a concatenated supermatrix (18S and 28S genes)
809 with bootstrap support values is displayed. All genera are represented as monophyletic clades.
810 *Panagrolaimus kolymaensis* is highlighted in red and basal to all other *Panagrolaimus* taxa.
811 Internal nodes, where all subsequent branches represent identical sequences, are displayed with
812 a black star. d) *P. kolymaensis* possesses *C. elegans* gene orthologs to enzymes required for
813 TCA cycle, glyoxylate shunt, glycolysis, gluconeogenesis, trehalose synthesis, and polyamine
814 synthesis. Black filled circles: Ortholog presence suggested by orthogroup clustering,
815 phylogenetic analysis, and domain architecture. White filled circles: No ortholog found via
816 current analysis. Coloured filled circles: Presence of *P. kolymaensis* gene(s), related to several
817 *C. elegans* genes (all genes of same colour) that are all co-orthologous to that gene (those
818 genes). Label: *C. elegans* enzyme names and orthogroup that contains that gene according to
819 our orthogroup clustering.
820
821
822
823
824
825
826
827
828
829
830
831
832
833

834 **Figure 4. *C. elegans* dauer larvae and *P. kolymaensis* utilize similar mechanisms to survive**
835 **cryptobiosis.**
836 a) Survival rate of *P. kolymaensis* nematodes to desiccation and freezing (-80°C). Error bars
837 indicate standard error of mean of two independent experiments with two technical replicates
838 performed on two different days. Statistical comparison was performed using unpaired t test
839 with Welch correction. n.s. $p > 0.05$, ****$p < 0.0001$. For desiccation (non-preconditioned) n
840 = 289, freezing (non-preconditioned) n = 675, desiccation (preconditioned at 98%RH) n = 953
841 and freezing (preconditioned at 98%RH) n = 1295. b) *P. kolymaensis* nematodes and *daf-*
842 *2(e1370)* dauer larvae upregulate trehalose levels upon preconditioning at 98%RH. Error bars
843 indicate standard error of mean of two independent experiments with three replicates
844 performed on two different days. Statistical comparison was performed using two-way
845 ANOVA with Holm-Sidak's multiple comparison test, ****$p < 0.0001$. c-d) 2D-thin layer
846 chromatography of ^{14}C-acetate labelled metabolites from *P. kolymaensis* that were non-
847 preconditioned and preconditioned at 98%RH. Enumerated spots indicate trehalose (1),
848 glucose (2), glutamate (3), glutamine (4), serine/glycine (5) and phenylalanine (6).
849 Representative images from at least two independent experiments performed on two different
850 days. e) Desiccated *daf-2 (e1370)* dauer larvae survive to freezing (-80°C) for an extremely
851 long period. Error bars indicate standard error of mean of two independent experiments with
852 two technical replicates performed on two different days. f) Brood size of desiccated dauer
853 larvae exposed to freezing remain like that non- desiccated dauer larvae. Average brood size is
854 the mean of seven dauer larvae per each condition. Statistical comparison was performed by
855 using non-parametric Kolmogorov-smirnov test n.s $p>0.05$.
856
857
858
859
860
861
862
863
864
865
866
867

Figure S1. Calibration of a radiocarbon (^{14}C) date.

Radiocarbon date (44,315±405 BP) and calibrated age (45,839 -- 47,769 cal BP) of plant material collected from buried borrow P-1320. Radiocarbon ages were converted to calendar age equivalents with the OxCal V.4.4 program using the IntCal20 calibration curve. Pink-shaded area — radiocarbon date with standard deviation; grey-shaded area — radiocarbon date projection on the calibration curve with 95.4% probability.

Figure S2. Morphology of *Panagrolaimus kolymaensis* sp. n., female.

Graphic presentations of holotype (a,b) and SEM pictures (c-i): a) anterior body, b) female reproductive branch, c–e) anterior end of three different female specimens, f) anterior part of the lateral ridge, g) vulva, h) ventral excretory/secretory pore, i) posterior body with anus and lateral ridge. Scale bars: a,b - 50 µm, c,i - 3 µm, d - 2 µm, e –1 µm, f,h - 5 µm, g - 10 µm, .

Figure S3. Phylogenies inferred for genes sets using both concatenation and coalescence approaches.

a) The ploidy level was analysed with *Smudgeplot* v0.2.1[70]. KMC version 3.1.0[71] was used to count the 21-mers in the PacBio CCS reads. Then we ran *smudgeplot.py* to determine the lower and upper coverage cut-offs. These were determined to be 14 and 380. 21-mers with a coverage between 14 and 380 were filtered with kmc_tools. Then, we computed the k-mer pairs from the filtered 21-mers by running *smudgeplot.py hetkmers*. Finally, the produced a smudgeplot shows an estimated ploidy of 3. b) Species tree inferred for 12,295 gene trees using a coalescence approach. The species tree implemented using the coalescence approach with orthogroup gene trees is displayed. Novel species in this study are displayed in red. All nodes have a posterior probability of 1. c) Species tree inferred for 102 taxa**.** The maximum likelihood tree inferred using a concatenated supermatrix of 60 genes is displayed. Bootstrap values are only displayed for nodes with less than 100% support. The platyhelminth *Macrostum lignano* serves as an outgroup for rooting. The ancestral *Panagrolaimus*, sister to all others within the *Panagrolaimus* genus, is highlighted in red.

Figure S4. Combination of cryptobiotic states enhances survival of *C. elegans* dauer larvae.

a) Desiccated dauer larvae manifest enhanced survival rate to heat stress (34°C). Error bars indicate standard deviation of two independent experiments with two technical replicates. b) Desiccated dauer larvae display enhances survival rate to anoxia. Error bars indicate standard deviation of two independent experiments with two technical replicates. Statistical comparison was performed by paired two tailed t-test. *$p<0.05$. c) *P. kolymaensis* possesses gene orthologs to most genes implicated in dauer formation and metabolism in *C. elegans*. Black filled circles: Ortholog presence suggested by orthogroup clustering, phylogenetic analysis, and domain architecture. White filled circles: No ortholog found via current analysis (in all cases these *C. elegans* genes did not cluster with any *Panagrolaimus* genes in the orthogroup clustering). Label: *C. elegans* enzyme names and orthogroup that contains that gene according to our orthogroup clustering.

1001 **Figure S5. *P. kolymaensis* reduces triacylglycerols (TAGs) levels and accumulates**
1002 **trehalose-6-phosphate upon preconditioning at 98%RH**.
1003 a) 1D-Thin layer chromatography of acetate labelled organic fractions of non-preconditioned
1004 (1) and preconditioned (2) *P. kolymaensis*. b) Mass spectrometric quantification of TAG levels
1005 of non-preconditioned (1) and preconditioned (2) *P. kolymaensis*. Error bars indicate standard
1006 deviation of two independent experiments with two technical replicates. Statistical analysis
1007 was performed using unpaired t-test with Welch correction **$p < 0.001$. c-d) non-
1008 preconditioned and preconditioned mass spectrum of an empty region, e-f) spot 1 (trehalose),
1009 g-f) spot 7 (trehalose-6-phosphate) scraped out and extracted from the 2D-TLC.
1010
1011
1012
1013
1014
1015
1016
1017
1018
1019
1020
1021
1022
1023
1024
1025
1026
1027
1028
1029
1030

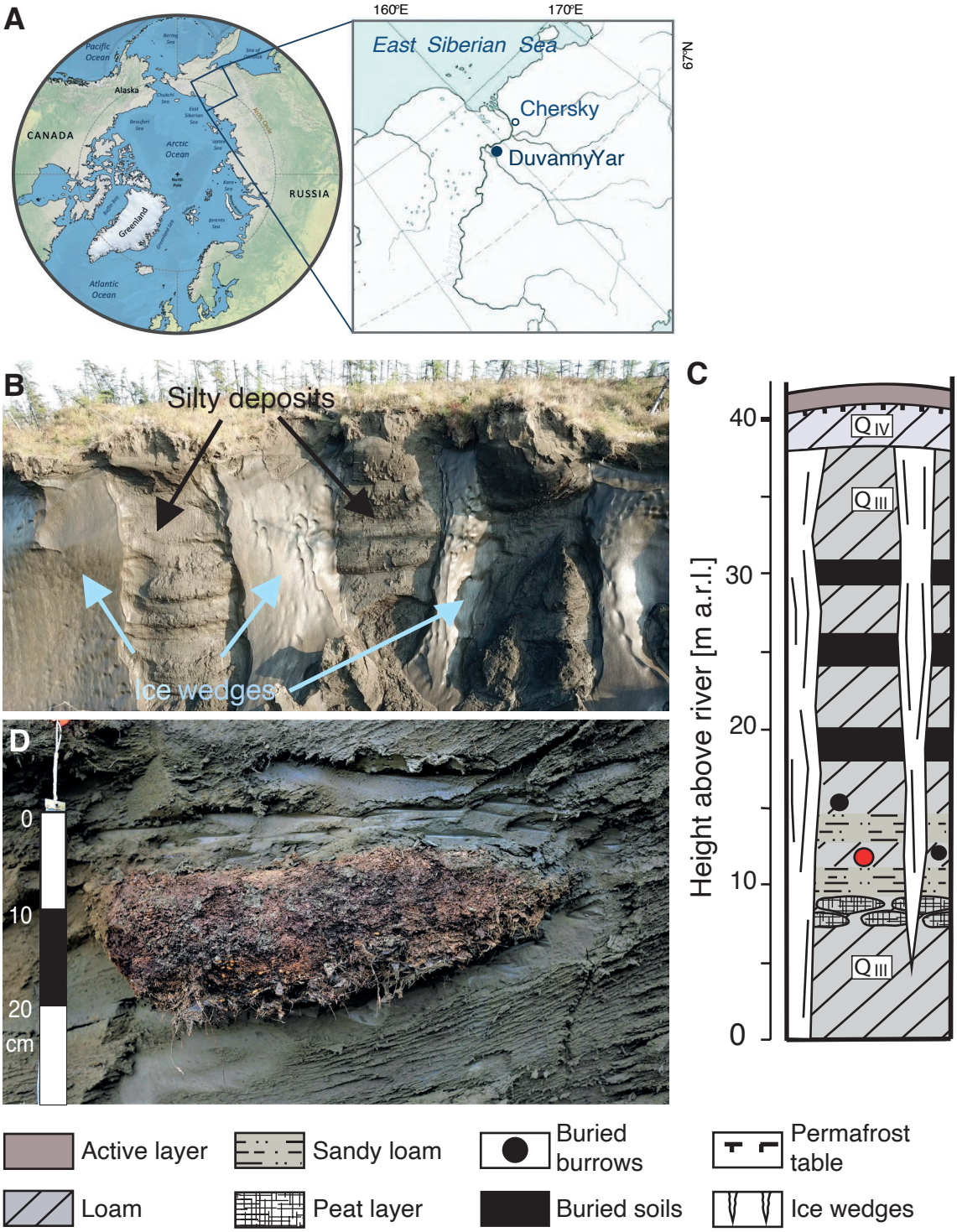

Figure 1
Shatilovich *et al*

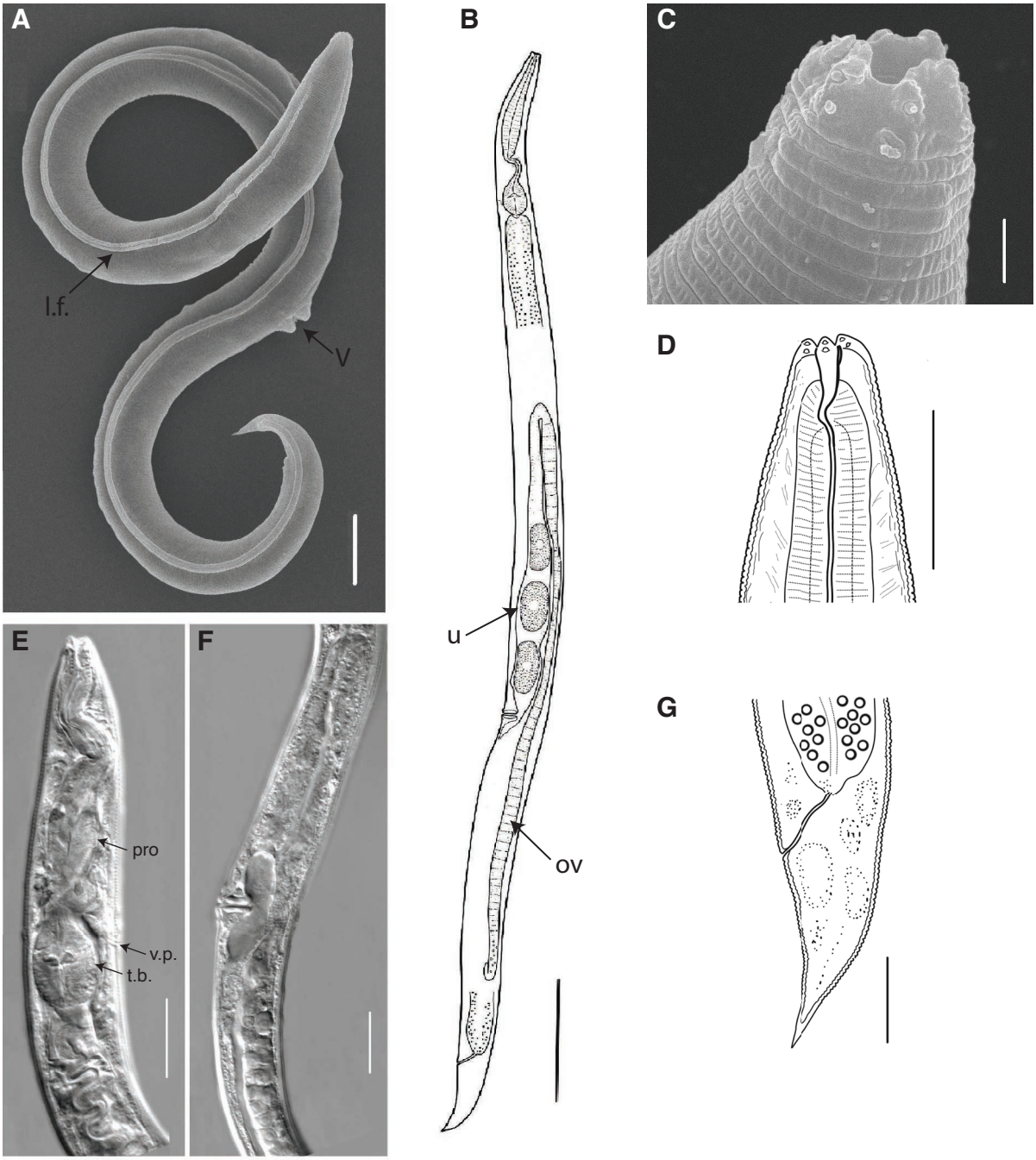

Figure 2
Shatilovich *et al*

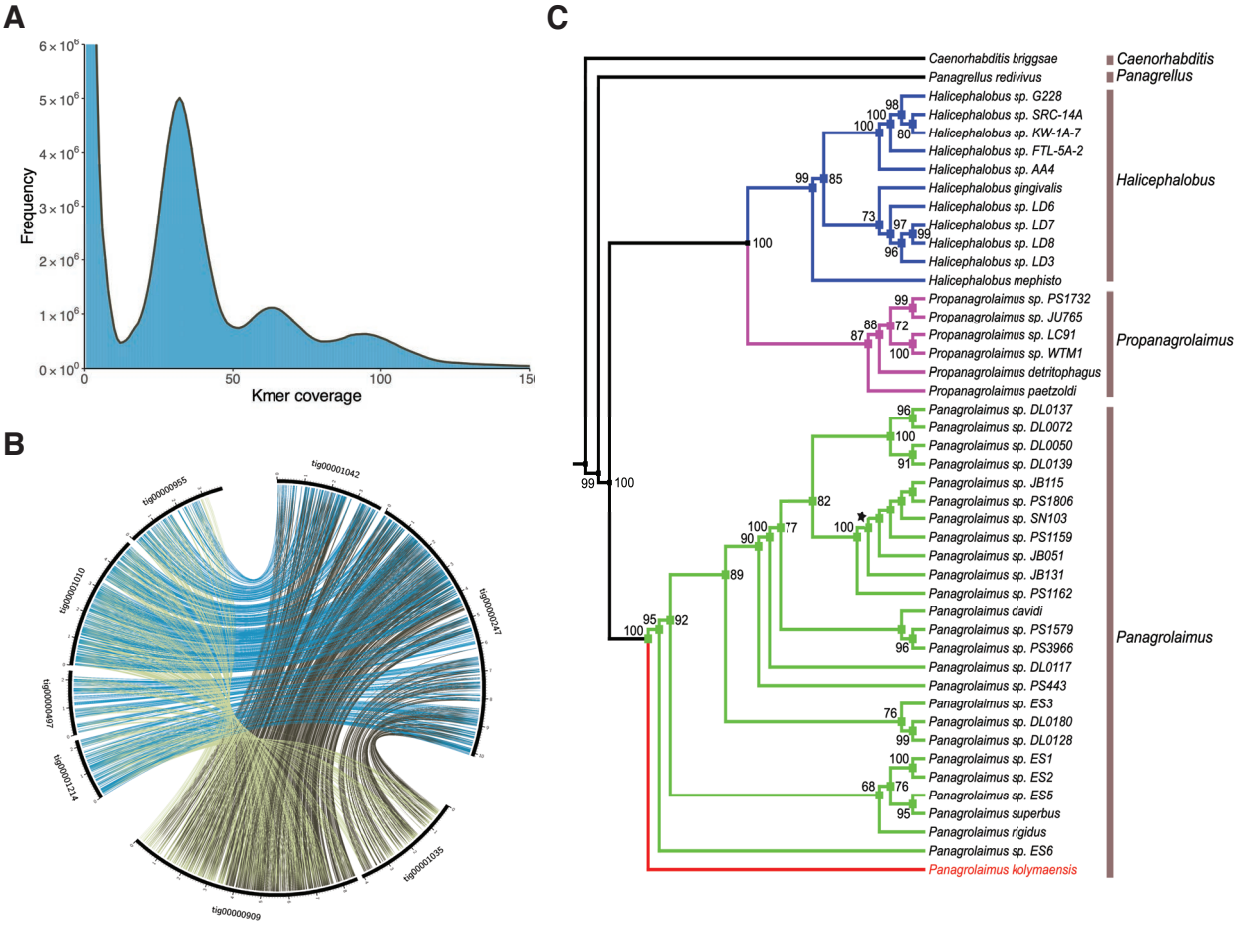

Figure 3
Shatilovich *et al*

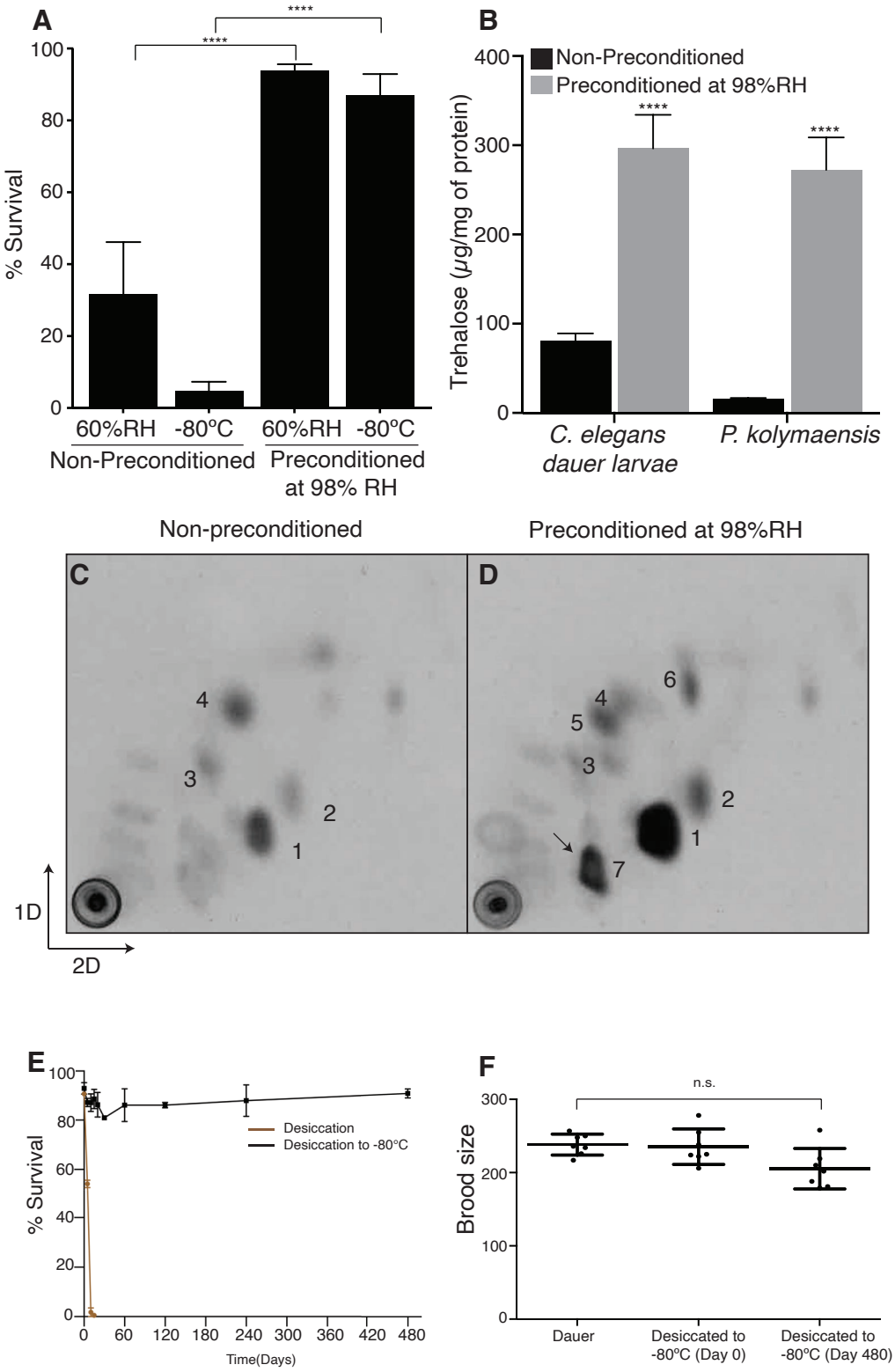

Figure 4
Shatilovich *et al*

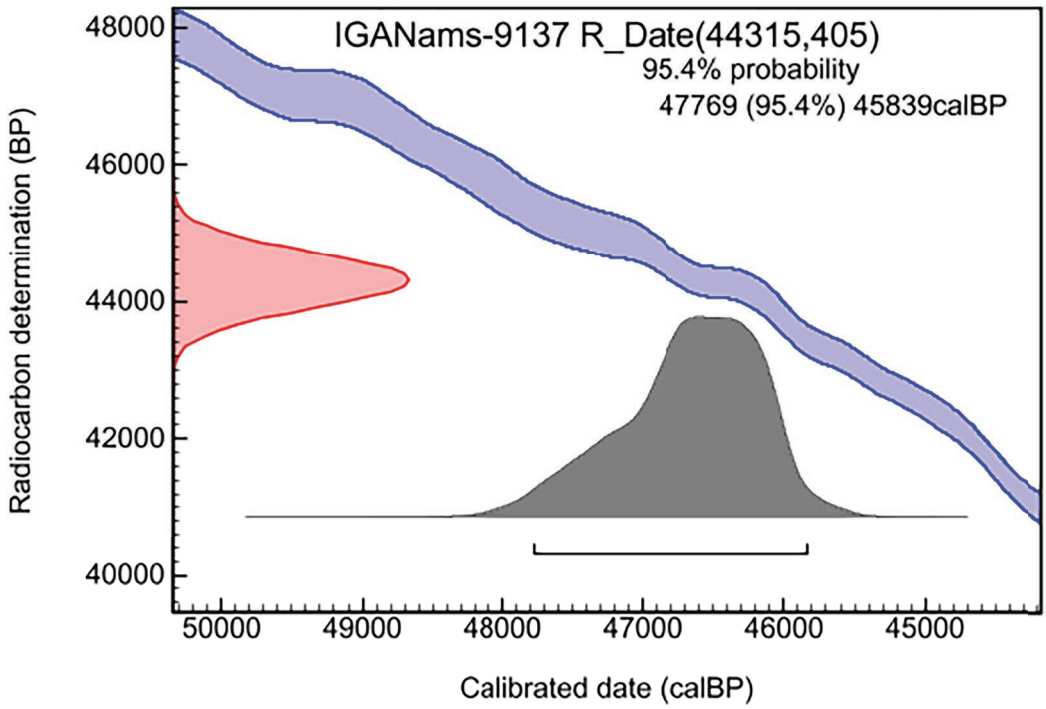

Figure S1
Shatilovich *et al*

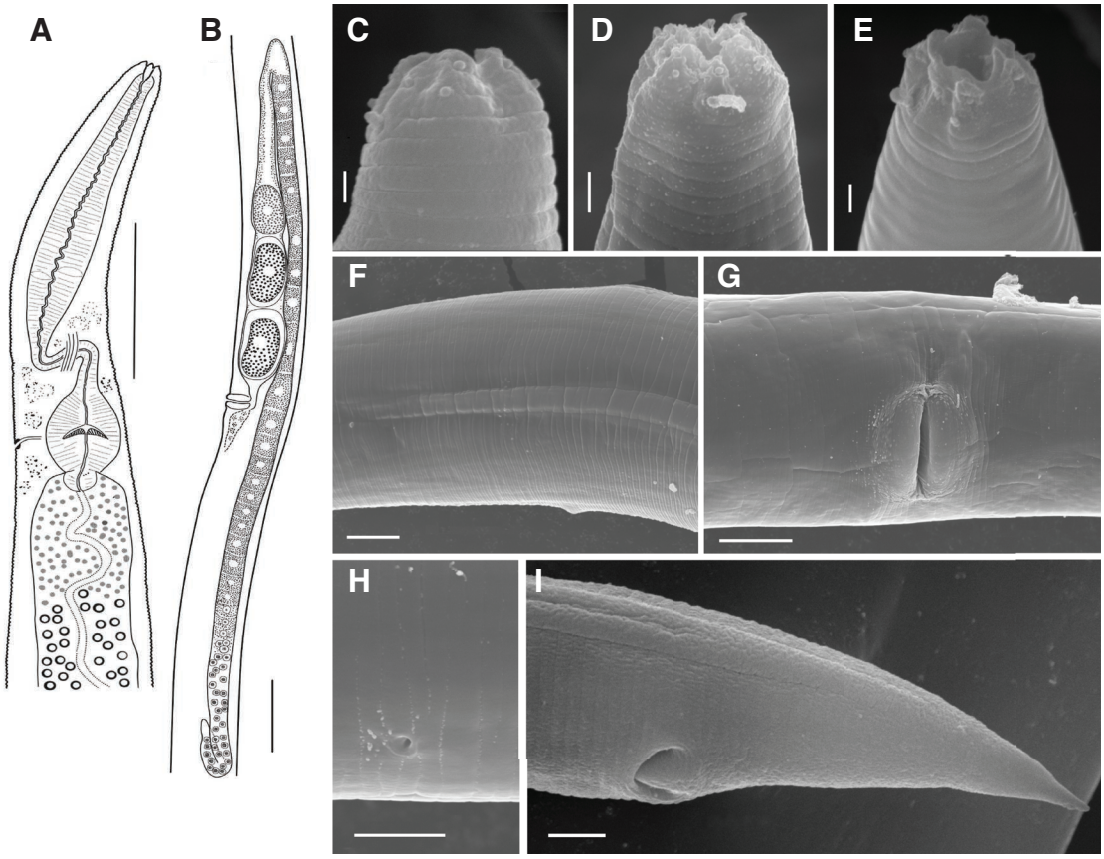

Figure S2
Shatilovich *et al*

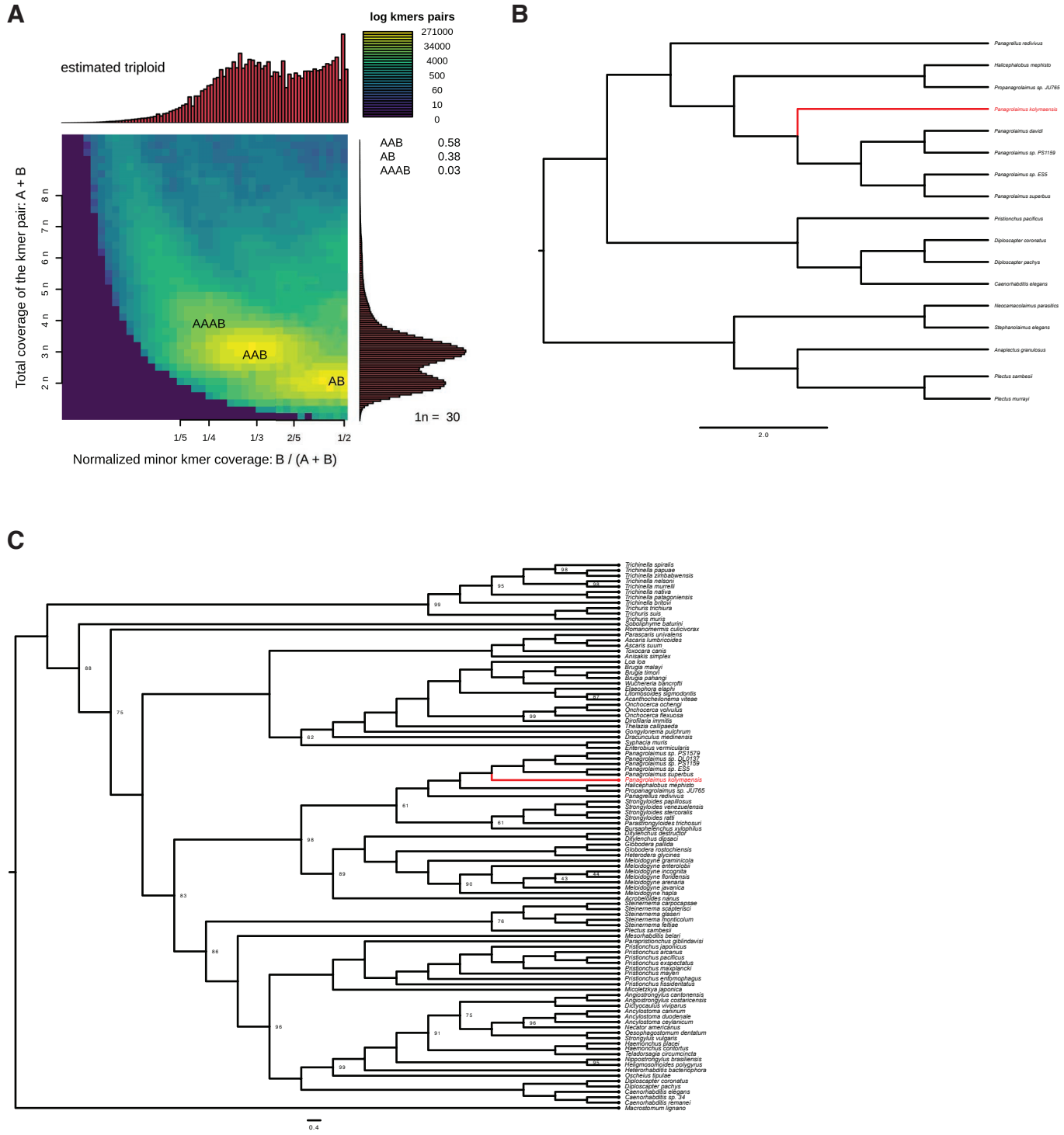

Figure S3
Shatilovich *et al*

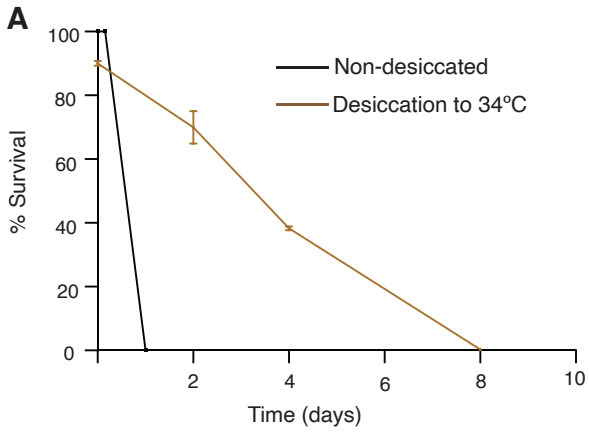

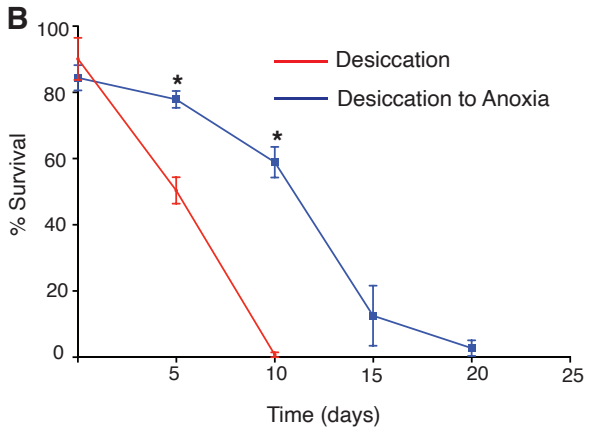

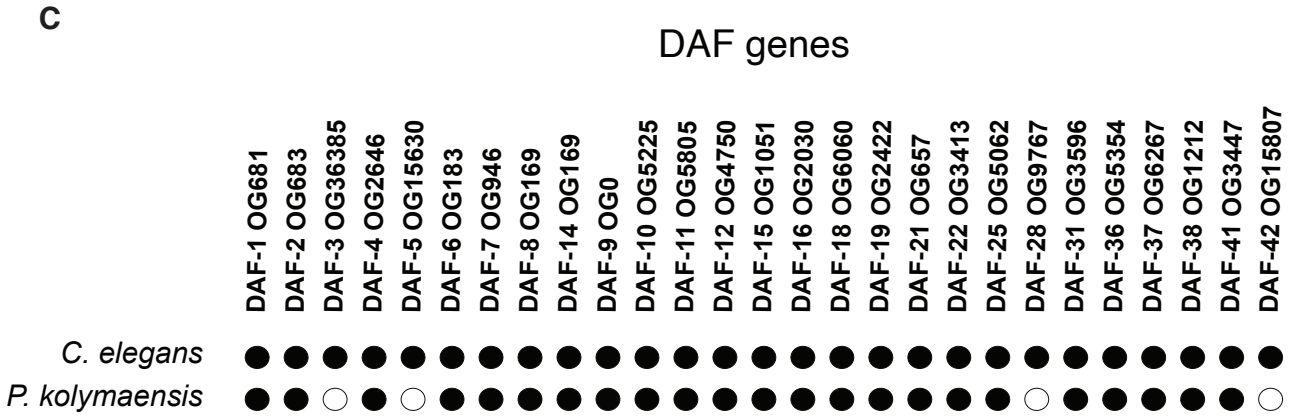

Figure S4
Shatilovich *et al*

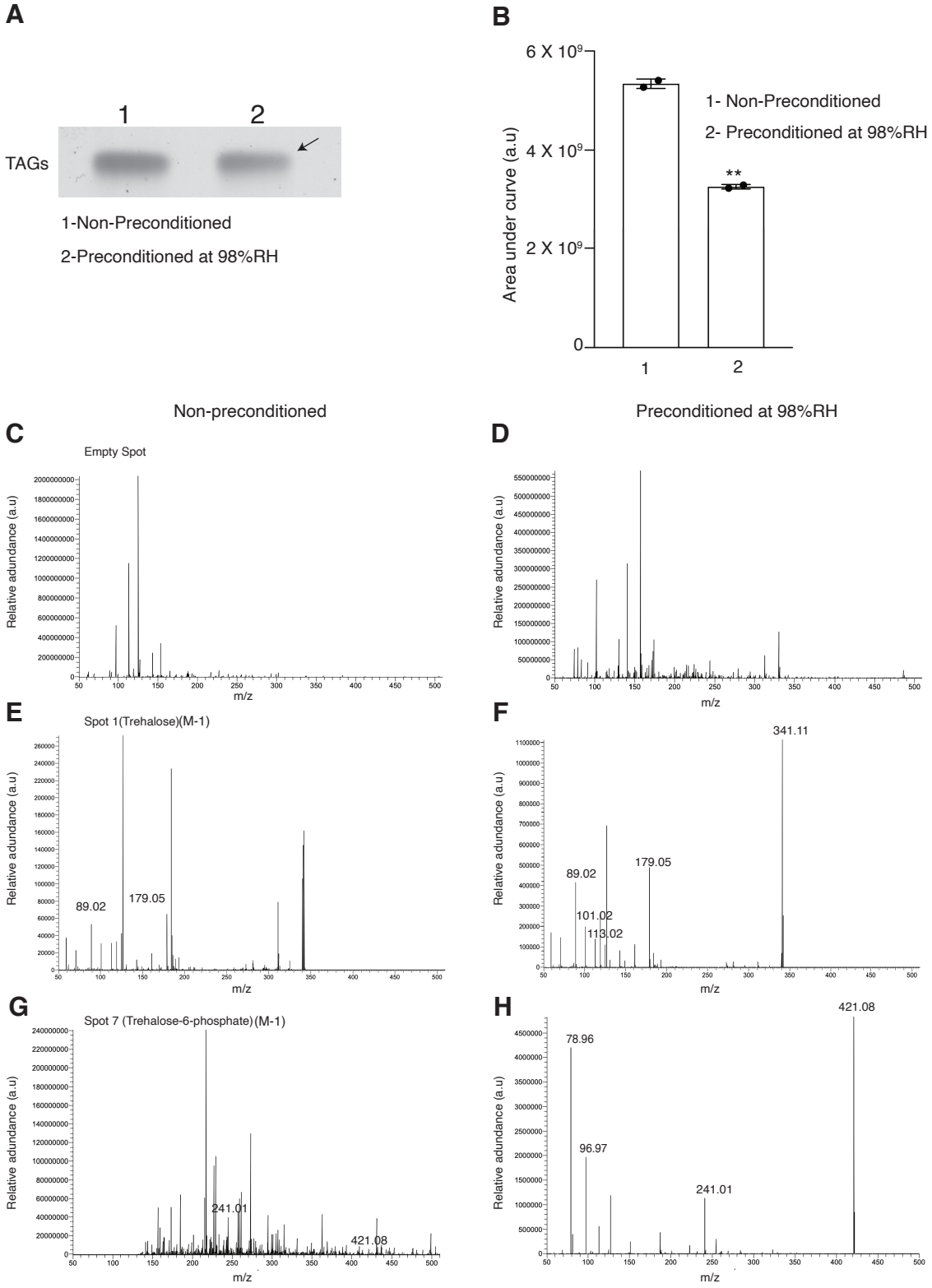

Figure S5
Shatilovich *et al*